RSC Advances

Charge-controlled switchable methane adsorption on heteroatom-doped BNNSs

Journal:	*RSC Advances*
Manuscript ID	RA-ART-10-2015-022537.R1
Article Type:	Paper
Date Submitted by the Author:	12-Dec-2015
Complete List of Authors:	Seif, Abdolvahab; university of kurdistan Azizi, Khaled; University of Kurdistane, Chemistry
Subject area & keyword:	Fossil fuels < Energy

Charge-controlled switchable methane adsorption on heteroatom-doped BNNSs

*Abdolvahab Seif and Khaled Azizi**

Department of Chemistry, University of Kurdistan, Sanandaj, Iran

**Corresponding author. Tel.: +98 871 6624133; fax: +98 871 6660075/+98 871 6624133.*

E-mail address: k.azizi@uok.ac.ir (K. Azizi)

Abstract

The adsorption behavior of methane (CH_4) on neutral and charged states of Al-, C-, P- and Si-doped boron nitride nanosheets (BNNSs), is investigated using density functional theory (DFT) method. The thermodynamic stability and structural parameters of all studied adsorbents in both cases of B atom replaced, X(B) and N atom replaced by doped atom, Y(N) (X or Y =Al, C, P, Si) were evaluated. It is found that replacing N atom from BNNS by Al (Al(N)) can notably enhance the adsorption energy (E_{ads}) of CH_4. Interestingly, it was shown that there is favorable charge-controlled switchable CH_4 storage on Al(B)-, Al(N)- and C(B)-BNNSs. According to the results, the CH_4 molecule can be effectively detected by Al(N)-BNNS. However, the more E_{ads}, flatness of the adsorbent sheet, and feasibility of synthesize turns the C(B)-BNNS to a promising material for CH_4 storage. The atom in molecules (AIM) methodology indicates that interaction of CH_4 with Al and C atoms in the mentioned systems is more effective, correlating with the more E_{ads} seen for these systems.

Keywords: Methane, Charge-controlled adsorption, Doped BNNSs, Gas adsorption, DFT, AIM

1. Introduction

One of the most important problems facing the world today is "Energy". In this regard, efficient energy storage systems are still highly controversial issue. Fossil fuels play an important

role in industrial, agricultural and urban life. Despite tremendous efforts to use clean fuels such as hydrogen, nowadays, the major amount of our desired energy is supplied through the huge fossil sources. However, efficient storage of these valuable sources has been known as a technological challenge.

Among energy sources, CH_4 (as the major component of natural gas) is of grate theoretical and practical interest.[1-4] Various theoretical and experimental researches have addressed the adsorption behavior of CH_4 on nanomaterial adsorbents.[5-7] In this regard it has been shown that pristine boron nitride nanotubes (BNNTs) have more potential related to their carbon counterparts for CH_4 adsorption,[8] although this partial enhancement is not enough for technical applications. On the other hand, it is well established that the local physical and chemical properties whereby the gas adsorption behavior of an intrinsic nanoadsorbent undergoes a significant change upon heteroatom doping. Recently it has been shown that Al-doped BNNTs can increase the adsorption energy of CH_4 up to 26 $kJ.mol^{-1}$.[9] However, the application of the NTs, and also other shapes of adsorbents such as fullerenes, has been mostly limited due to the unavailability of their inside surfaces.

Nanosheets (NSs) have attracted much attention due to their wide available surfaces and various mechanical and electronic properties. It has been demonstrated that similar to the NTs, heteroatom doping can effectively improve the gas adsorption potential on the NSs.[10] For instance, using DFT calculations it has been shown that, while CO molecule was found to be weakly adsorbed onto the pristine graphene, Al-doped graphene strongly chemisorbed CO molecule.[11] This is also right for hydrogen physisorption on B, Ti, Zn, Zr, and Al-doped graphene sheets.[12]

Besides graphene sheets, it has been found that the properties of mono atomic layered BN sheets are strongly dependent on the dopants.[13] For example, DFT calculations indicated that the Al(B)-BNNS is a promising material for hydrogen storage.[14] Furthermore, the CH_4 adsorption on pristine and Al-doped states of graphene along with pristine BNNS has been recently explored using DFT calculations.[15,16] However, the adsorption of CH_4 on heteroatom-doped BNNSs has not been reported yet, either theoretically or experimentally.

The significant enhancement of gas adsorption properties of nanostructures by variation of charging state has already been proven.[17,18] It is important to note that charging the systems can be realized by different approaches including electrochemical, electrospray, gate voltage control and electron beam methods.[19]

In this work, the adsorption behavior of CH_4 molecule on Al, C, Si and P-doped BNNSs is investigated using DFT method. Due to the lack of experimental data and in order to providing a more realistic evaluation of the adsorption properties of heteroatom-doped BNNSs with respect to CH_4, single point (SP) calculations have been carried out by using two different functionals within DFT. We have also studied the effect of electron injecting (e^-) and removing (e^+) charge states of pristine and heteroatom-doped BNNSs on the CH_4 adsorption quality. The results were additionally analyzed by partial density of state (PDOS) profiles. Finally, AIM analysis was carried out in order to gain further insight into the nature of interactions between CH_4 and flakes.

2. Computational details

In this work, a BN sheet made by 25 B and 25 N atoms was selected as primer adsorbent. To avoid boundary effects and have the same edges effects, 5 H atoms were located on each edge (totally 20 H atoms). Furthermore, substitution of both B and N atoms from nanosheet was

carried out by each of Al, C, P and Si heteroatoms. The central locations on these flakes substituted by the heteroatoms are named as X(N) and Y(B) (Figure 1).

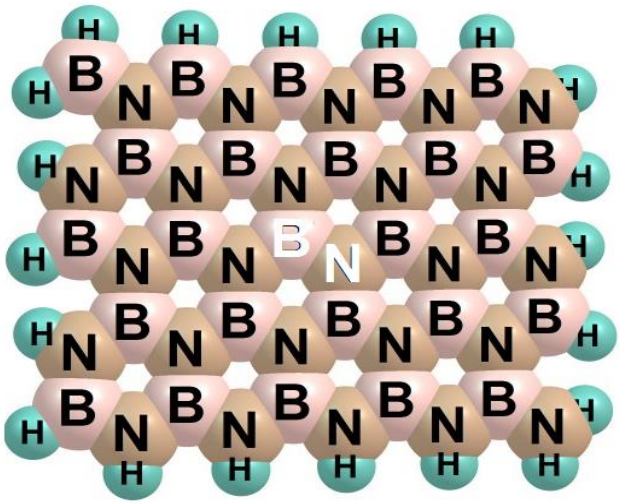

Fig. 1. Schematic graph of BN sheet by the representation of sites of X(N) and Y(B) in which X and Y letters refer to the locations for substitution of doped heteroatoms.

All geometry optimization and single point (SP) calculations were performed by using DFT method as implemented in GAMESS suite of program.[20] In this work we used 6-311G(d,p) basis set along with exchange–correlation functional of Perdew and Wang (PW91),[21] which has been distinguished to be suitable for the estimation of nonbonding interactions[22, 23] for the geometry optimization of nanostructures. Harmonic vibrational frequency calculations at the same level were carried out to confirm that the obtained structures corresponded to real minima. The electronic properties and the SP calculations have been performed at the modified exchange-correlation functional of Perdew and Wang (MPW1PW91)[24, 25] and M06-2X functionals with the same basis set. It should be mentioned that the MPW1PW91functional has been well described interaction between CH_4 and BN structures.[9] Also M06-2X functional was found to be a good descriptor of non-covalent interactions and its results are in good agreement with experimental

data.[26] The values of E_{ads} are calculated from the energy difference between the reactants (BNNSs and the CH_4 molecule) and BNNS/CH_4 complex product species. Regarding this definition, $E_{ads}<0$ could be referred for effective adsorption of CH_4 by adsorbent. In addition, the adsorption energy of each system was computed within the same charge state and was also corrected for the basis set superposition error (BSSE). The electrostatic charge distribution (EDD) and the amount of charge transfer between moieties were obtained using the scheme proposed by Mertz *et al.*[27] The energy gap variation, ΔE_{gap}, for any BNNS/CH_4 complex is defined as $\Delta E_{gap}=E_{gap(sheet-CH4)}-E_{gap\ (sheet)}$, where E_{gap} is the difference between the energies of the highest occupied molecular orbital, HOMO, and the lowest unoccupied molecular orbital, LUMO. The PDOS of the pristine and the gas-adsorbed nanosheets were visualized by the GaussSum program.[28] Finally, the AIM theory[29] has been used to analyze the nature and the strength of interactions between moieties by the AIM2000 program.[30]

3. Results and discussion

3.1. Structural and electronic analysis of BNNSs

The calculated structural and electronic properties of isolated BNNSs are summarized in Table 1. As can be seen from this table, except for C-doped BNNSs, doping pulls the substituted heteroatom out of the sheet surface. This leads to a significant change in local geometry around the substitution place on the sheet. The effect can be explained by the fact that the Al, Si and P atoms, belonging to the third row of the periodic table, have the larger atomic radius compared to the B, N and C atoms. Accordingly, as can be seen, the maximum protrusion has been obtained for the Al(N) case with the largest atomic radius. However, the B-replaced case of all doped systems, aside from C-doped ones, has the smaller protrusion indicating the formation of bonds with more ionic nature between doped atom and its neighbors. Inspection of the geometrical

properties of the studied sheets reveals also that for the equilibrium distance around dopants position, Y(B)-BNNSs have the smaller bond length than those of X(N) ($r_{N-Y}<r_{B-X}$). This can be attributed to the smaller atomic radius of N atom related to the B counterpart and also the more ionic nature of the N-Y bond compared with the B-X one for the same dopant (when X and Y are the same atoms).

Since almost all of the heteroatom doped BNNSs used in this study have not been synthesized so far, here we investigate some aspects of the thermodynamic stability of these flakes. The results of the vibrational calculations for the relative amount of the Gibbs free energies ($\Delta G_{form,\,r}$) at 298 K of the following reaction are given in Table 1,

$$n_B B(g) + n_N N(g) + n_H H(g) + HA(g) \rightarrow HA(Z) - BNNS(g) + Z(g)$$

where HA and Z stands for doped heteroatom and replaced atom from BNNS (B or N), respectively. n_B, n_N and n_H indicate the number of B, N and H atoms in BNNS system, respectively. As can be seen, the estimated values of $\Delta G_{form,r}$ are reasonable, such that the minimum values are obtained for pristine and C-doped BNNSs, respectively.[31, 32] Although, the $\Delta G_{form,\,r}$ values of all doped BNNSs are positive, however, it should be remembered that these values are compared with respect to the empirically stable BNNS.[33,34]

To have a clear understanding of the effect on the adsorption of CH_4, structural and electronic properties including dipole moment, HOMO-LUMO energy gap of flakes along with hybridization and electrostatic charge of doped atoms are also presented in Table 1.

Table 1. The structural and electronic properties of the heteroatom–doped BNNSs.

	P (Å)[a]	X-Y distance (Å)	$\Delta G_{form,\ r}$ (kcal.mol^{-1})[b]	ICS[c]	DM (D)[d]	H[e]	ECTA (|e|)[f]		E_{gap} (eV)[i]	
System	B3PW91	B3PW91					MPW[g]	M06[h]	MPW	M06
BNNS	0.0	1.44	0.0	0	5.71	$sp^{2.56}$	-0.483	-0.470	6.020	8.181
1e-				-1	24.30	$sp^{2.79}$	-0.357	-0.261	0.533	1.300
1e+				+1	16.56	$sp^{2.50}$	-0.513	-0.477	7.146	8.181
Al(B)	1.04	1.74	124.0	0	5.80	$sp^{2.56}$	1.370	1.370	6.041	8.221
1e-				-1	17.74	$sp^{2.71}$	0.884	0.86	0.633	1.381
1e+				+1	39.91	$sp^{2.55}$	1.230	1.22	0.695	1.468
Al(N)	2.10	2.05	325.6	0	5.91	$sp^{2.56}$	0.942	0.93	2.588	4.307
1e-				-1	6.93	$sp^{2.58}$	-0.013	-0.57	1.791	3.221
1e+				+1	9.52	$sp^{2.55}$	1.135	1.13	1.577	3.123
C(B)	0.00	1.41	23.1	0	5.83	$sp^{2.56}$	0.237	0.235	2.347	3.628
1e-				-1	11.84	$sp^{2.67}$	0.242	0.218	0.791	1.951
1e+				+1	3.42	$sp^{2.49}$	0.541	0.583	3.890	6.013
C(N)	0.00	1.52	58. 6	0	5.81	$sp^{2.51}$	-0.098	-0.081	3.300	5.430
1e-				-1	4.76	$sp^{2.58}$	-0.335	-0.372	2.671	4.496
1e+				+1	8.00	$sp^{2.49}$	0.052	0.165	1.145	2.692
P(B)	1.36	1.72	96.86	0	5.89	$sp^{2.56}$	0.032	0.058	5.309	7.312
1e-				-1	25.54	$sp^{2.86}$	1.390	1.415	0.559	2.402
1e+				+1	4.16	$sp^{2.49}$	1.670	1.752	0.782	3.242
P(N)	1.69	1.96	151.3	0	5.96	$sp^{2.56}$	-0.373	-0.388	6.027	8.020
1e-				-1	14.19	$sp^{2.71}$	-0.504	-0.559	0.514	1.203
1e+				+1	7.87	$sp^{2.55}$	-0.178	-0.188	0.721	2.097
Si(B)	1.36	1.73	82.4	0	5.85	$sp^{2.56}$	0.298	0.366	4.662	6.530
1e-				-1	10.05	$sp^{2.60}$	-1.022	-1.066	1.097	2.658
1e+				+1	4.37	$sp^{2.49}$	1.169	1.287	1.393	3.278
Si(N)	1.87	1.89	219.7	0	5.84	$sp^{2.56}$	0.225	0.253	3.136	7.159
1e-				-1	6.91	$sp^{2.58}$	-0.480	-0.514	2.269	3.884
1e+				+1	8.18	$sp^{2.55}$	1.147	1.283	0.910	2.666

[a] Protrusion of heteroatom from the entire sheet plane.

[b] Relative Gibbs free energy of formation with respect to that of pristine BNNS.

[c] Injected charge state.

[d] Dipole moment in Debye calculated at the M06-2X method.

[e] Hybridization of heteroatom.

[f] Electrostatic charge on target atom.

[g] MPW1PW91.

[h] M06-2X.

[i] HOMO-LUMO energy gap.

Comparing the results of the charges indicate that these values follow the same pattern, Table 1. As illustrated, the absolute values of charge on dopant in each system are nearly identical for both MPW1PW91 and M06-2X computational methods, whereby the largest absolute amount of the charge in the neutral systems is upon the Al atom in the Al(B)-BNNS. In addition, the results show that they are strongly dependent on the position of substitution, thus their values for Y(B) cases are more positive than those of X(N) (because of the more electronegativity of the N atom in compare with the B atom).

In this work in order to find an efficient way to improve the adsorption capacity of CH_4, the effects of injection and removing of charge on the adsorption properties of BNNSs were also studied. As shown in Table 1, while the charge on the N atom becomes slightly more positive in both $1e^-$ and $1e^+$ states of pristine BNNS, the positive charge on the dopant, respectively decreases and increases in the $1e^-$ and $1e^+$ states in all doped BNNSs.

Inspection of the values of E_{gap} (Table 1) for all the studied neutral sheets reveals that the results of MPW1PW91 functional are more realistic than that of M06-2X, regarding the reported experimental E_{gap} of pristine BNNS (~5-6 eV).[31]

According to the results, except for C(B)-BNNS/$1e^+$, the amount of E_{gap} decreases for all the sheets after the injection or removing of charge. The reduction of E_{gap} according to the Koopmans' approach,[35] may lead to the more chemical reactivity of BNNSs and increasing of tendency of this flakes to interact with foreign chemical species.

3.2. Methane adsorption process

3.2.1. Geometries and energies of adsorptions of methane on neutral BNNSs

Next, we investigated the interaction between CH_4 and BNNSs. Different geometries including above the either hetero atom and the center of hexagon rings including the Al, C, P and

Si atoms (for the pristine case, X and Y positions) were selected as initial configurations of the CH_4 on the surface of BNNSs. In addition, in order to obtain the more stable position, in each mentioned configuration we have chosen the CH_4 molecule on three sides, in which one, two and three H atoms of CH_4 were oriented toward the surface of nanosheets. Figure 2 shows the most stable configuration of adsorbent/CH_4 systems for pristine (a) and doped (b-e) sheets. A closer look at this figure clarifies that, in exception of the Al-doped cases, CH_4 molecule is interacted with the surface of sheets via one H atom. In both Al(B)-BNNS/CH_4 and Al(N)-BNNS/CH_4 states, the adsorbed CH_4 molecule prefers to have a configuration with a favorable electrostatic interaction between negative charge on the C atom of CH_4 and the positive charge on the Al atom. It should be noted that such a configuration, despite considerable amounts of positive charges on dopants, has been not selected by P(B)-BNNS/CH_4 and Si(B)-BNNS/CH_4 systems.

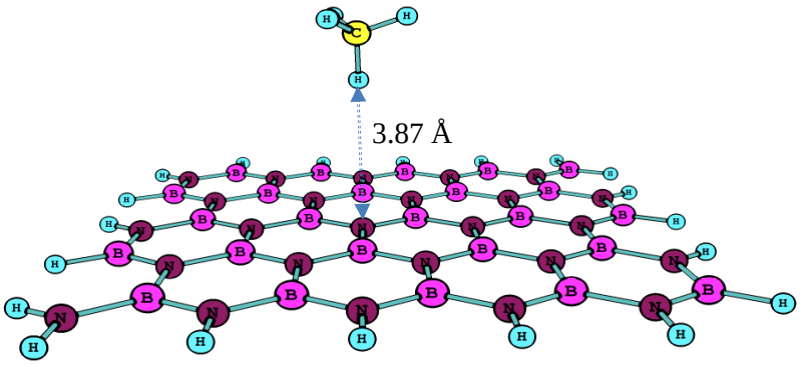

(a) BNNS/CH_4

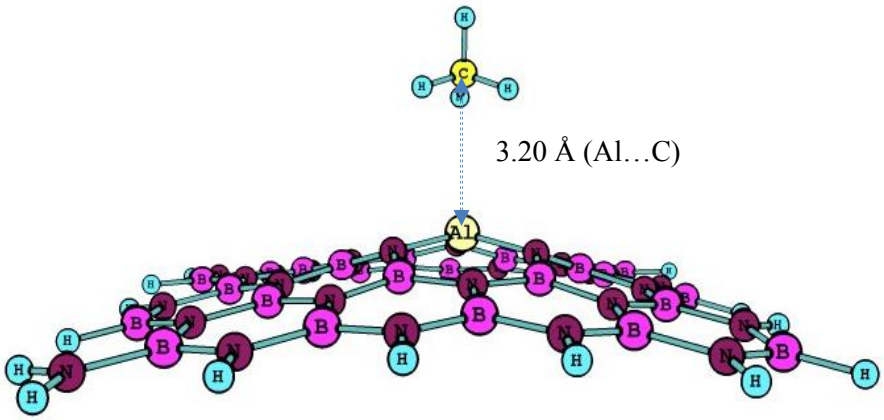

(b1) Al(B)-BNNS/CH_4

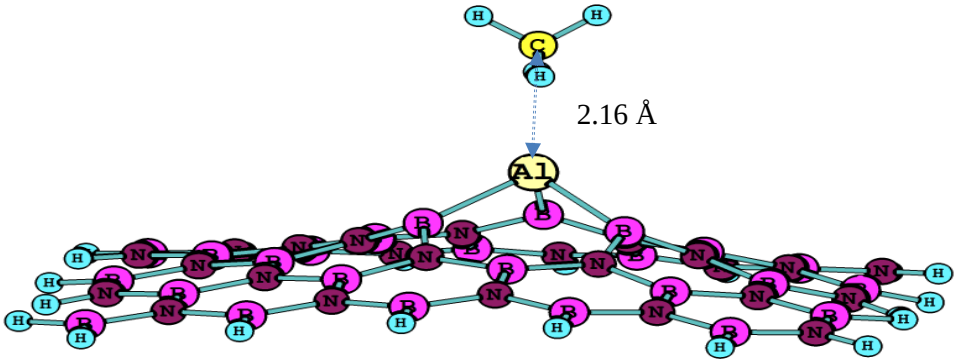

(b2) Al(N)-BNNS/CH_4

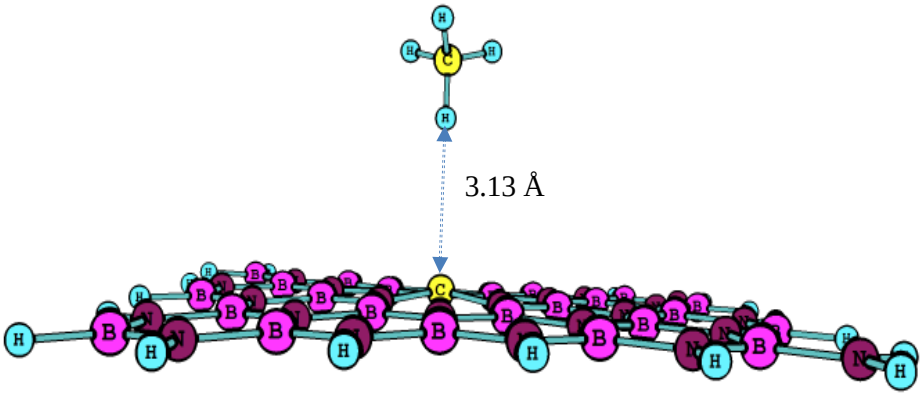

(c1) C(B)-BNNS/CH_4

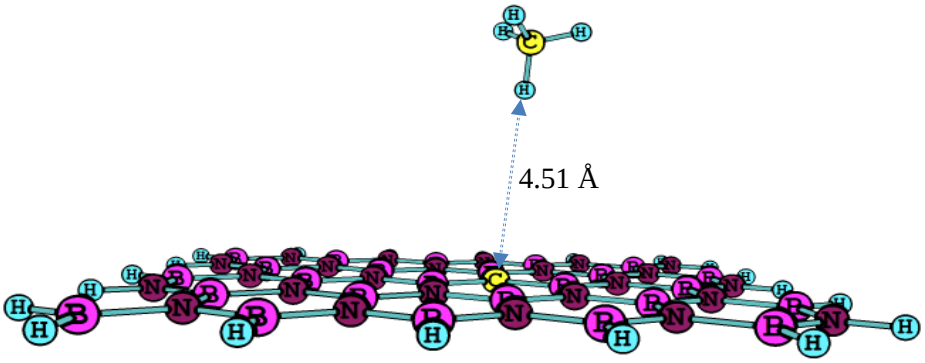

(c2) C(N)-BNNS/CH_4

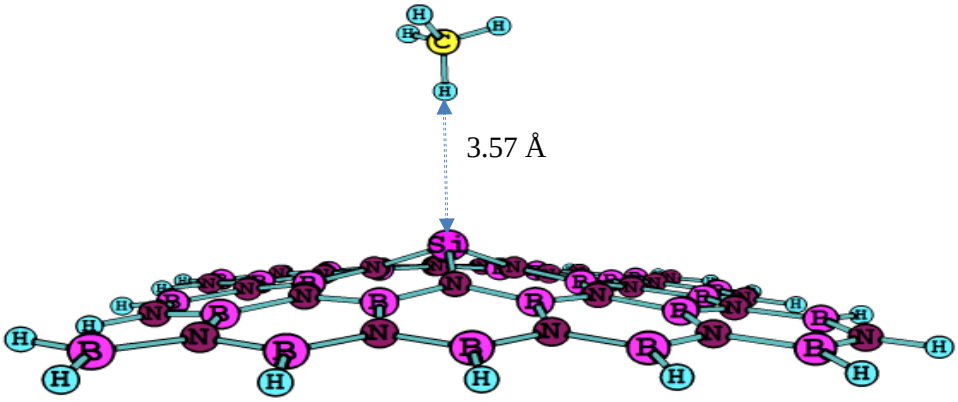

(d1) Si(B)-BNNS/CH_4

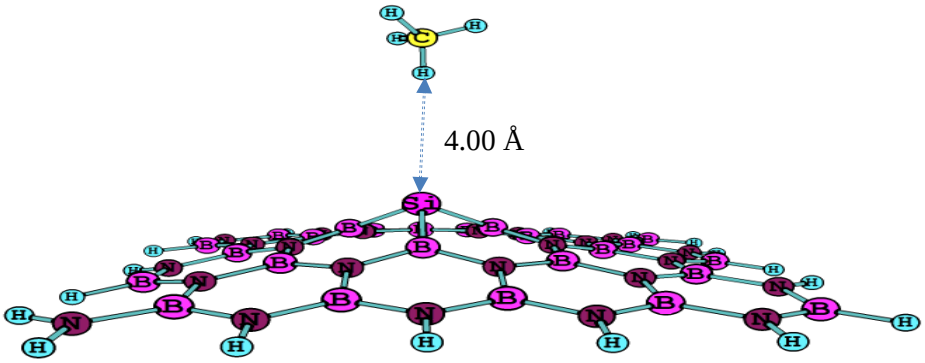

(d2) Si(N)-BNNS/CH_4

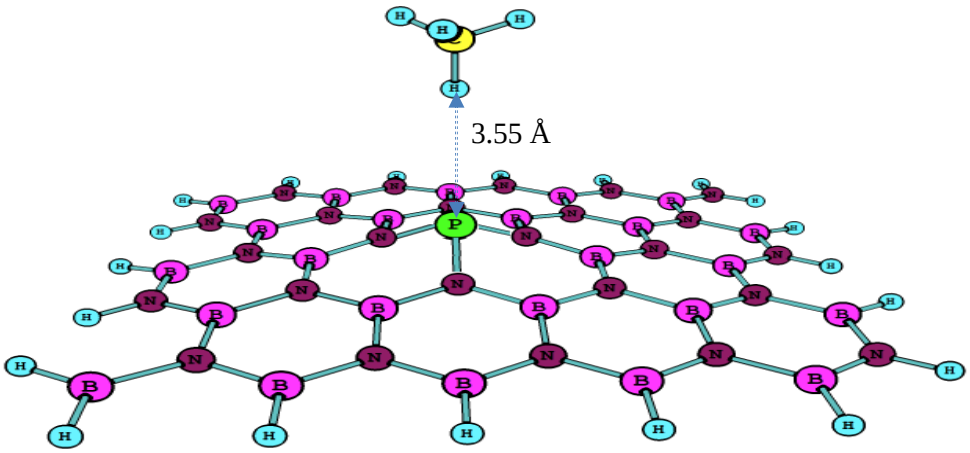

(e1) P(B)-BNNS/CH_4

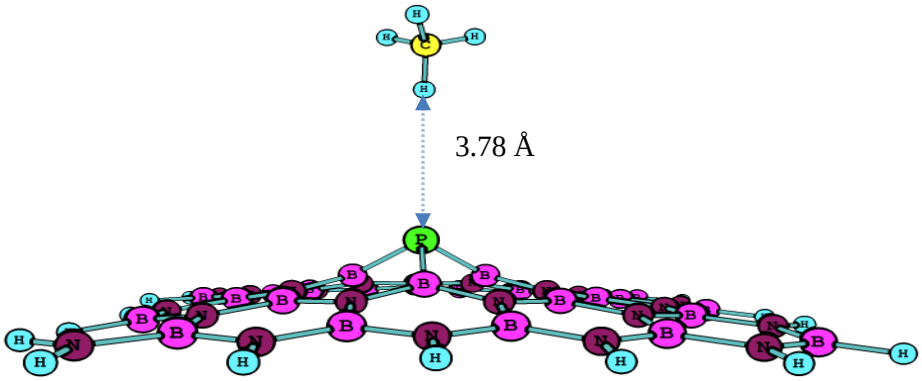

(e2) P(N)-BNNS/CH_4

Fig.2. The most stable configurations of adsorbed CH_4 on the surface of BNNSs; (a) pristine, (b) B(b1) and N(b2) atoms of sheet replaced by Al atom, (c) B(c1) and N(c2) atoms of sheet replaced by C atom, (d):B(d1) and N(d2) atoms of sheet replaced by Si atom and, (e):B(e1) and N(e2) atoms of sheet replaced by P atom. The nearest distance between the CH_4 and the surface of BNNS are also specified for each system.

The E_{ads} values of CH_4 on the pristine and doped BNNSs are reported in Table 2. To the best of our knowledge, the E_{ads} of CH_4 over BNNS flakes has not been experimentally reported yet. Thus, in order to increase the validity of the obtained results, two different functionals within DFT (MPW1PW91 and M06-2X method) were used for calculation of E_{ads}. According to the

obtained results of both functionals, in contrast with the previously reported results,[16] CH_4 cannot effectively bind (E_{ads}~2 kJ.mol^{-1}) to the surface of the pristine BNNS.

To achieve a good adsorption of CH_4 on BNNSs, we used the Al, C, Si and P atoms as dopant. It is clear from our findings that the Al doping provides the largest amount of E_{ads}, in the range of 15-28 kJ.mol^{-1} (at the M06-2X method). This feature indicates that both Al(B)-BNNS and Al(N)-BNNS states have remarkable potential for CH_4 storage. It is noteworthy to mention that, as in the case of BNNTs,[9] the Al(N)-BNNS/CH_4 shows the larger E_{ads}, roughly 12 kJ.mol^{-1} (at the M06-2X method) than that Al(B)-BNNS/CH_4 system. The difference in E_{ads} of CH_4 on two cases could not be justified by the amounts of positive charges on the Al atom in two cases. It is interesting to mention that while the orientation of CH_4 to the surface of the Al-BNNSs is determined by the electrostatic forces, the main contribution to the adsorption energy is owned by dispersion forces. The results also clarify that, because of low adsorption energies, the neutral C- P- and Si-doped BNNSs cannot be suitable for the CH_4 storage. As shown by Table 2, CH_4 does not adsorbed properly on relatively unstable Si(N)-BNNS system, therefore, strong adsorption of CH_4 to the Al(N)-BNNS should not be simply accounted for the thermodynamic instability of this system.

3.2.2 The effects of charging of BNNSs on methane adsorption

In order to improve the CH_4 adsorption on BNNSs, effects of injection or removing of charge were studied on these systems (Table 2). Regarding to the results, electrical charging either by $1e^-$ or $1e^+$ has no evident effect on the E_{ads} of CH_4 on the pristine BNNS. On the other hand there is a good charge-controlled switchable CH_4 storage using the Al(B)-, Al(N)- and C(B)-BNNS systems. This suggests that the quality of the adsorption of CH_4 can be altered by the electrical charging of these systems. More importantly, consider that the CH_4 molecule shows ineffective

interactions with neutral C(B)-BNNS and is weakly adsorbed. When additional electrons ($1e^-$ and $2e^-$) are injected into C(B)-BNNS, CH_4 molecule becomes tightly bound and firmly adsorbed. Regarding to the considerable amount of E_{ads} in $2e^-$ state and the flatness of the sheet, CH_4 could be adsorbed by both sides of C(B)-BNNS system. This finding along with empirical reproducibility turns the C(B)-BNNS to a promising material for the CH_4 storage.

Table 2. Adsorption energies ($kJ.mol^{-1}$) of CH_4 adsorbed on BNNSs at the MPW1PW91 and the M06-2X methods

	Charge state					
	0		-1		+1	
System	MPW1PW91	M062X	MPW1PW91	M062X	MPW1PW91	M062X
BN/CH_4	-2.12	-2.07	-1.70	-1.63	-2.57	-2.07
$Al(B)/CH_4$	-6.44	-15.82	14.27	7.62	-10.44 (1451.5)[a]	-19.86 (1514.1)
$Al(N)/CH_4$	-24.96	-28.46	47.74	48.19	-45.80 (-66.66)	-49.88 (-78.73)
$C(B)/CH_4$	-5.44	-9.75	-17.49 (-37.04)	-28.25 (-53.31)	39.24	38.25
$C(N)/CH_4$	-0.45	-0.87	-2.14	-2.65	-0.65	-1.13
$Si(B)/CH_4$	-1.62	-2.64	-8.76	-9.45	-3.28	-4.13
$Si(N)/CH_4$	-0.39	-0.80	-3.14	-3.40	-1.20	-1.53
$P(B)/CH_4$	-1.47	-1.85	-2.28	-1.96	-1.99	-2.67
$P(N)/CH_4$	-1.00	-1.44	-2.31	-1.74	-0.88	-2.33

[a] The values given in parenthesis refer states of +2 and -2 electrical charging.

It is interesting that by reversing the circuit and removing of one electron ($1e^+$ state), the CH_4 molecule spontaneously desorbs from the surface of C(B)-BNNS. Accordingly, the idea of "charge-controlled switchable CH_4 adsorption" on C-doped BNNSs is technically important and can be considered for further studying as one of the efficient ways for the CH_4 storage. The results demonstrate that there is an inverse trend, with respect to C(B)-BNNS/CH_4, in Al(B)- and Al(N)-BNNS/CH_4 systems, whereby in $1e^-$ state, CH_4 molecule spontaneously desorbs from the surface of absorbent. Therefore, as in the case of C(B)-BNNs/CH_4, a good charge-controlled switchable CH_4 storage, especially for Al(N)-BNNS/CH_4 system is predicted. However, the

removing of charge has different effects on Al(B)-BNNS/CH_4 and Al(N)-BNNS/CH_4 systems. While the removing of $1e^-$ increases E_{ads} of CH_4 on both cases, CH_4 is strongly desorbed and adsorbed by $2e^+$ state of Al(B)-BNNS and Al(N)-BNNS systems, respectively. Remarkably, the $2e^+$ state of Al(N)-BNNS system with the maximum amount of E_{ads} (-78.73), is estimated to be the most suitable case among studied BNNSs for the CH_4 adsorption. It may adsorb several CH_4 molecules per any Al-doped position. The results show also that some remarkable differences between the values of adsorption energies (especially in the Al(B) and C(B) cases), Table 2. This can be attributed to the specific formulation of the two functional used in this work. As can be seen, electrical charging process (either injection or removing) has no evident effect on the E_{ads} of CH_4 on the BNNSs doped by the atoms of P, Si and C in N- replaced cases. Although Si(B)-BNNS/CH_4 system at $1e^-$ and $2e^-$ states shows a moderate E_{ads}, this amount of adsorption energy smaller than that could be considered for technical applications.

The charge transfer process between moieties has been also explored (Table 3). This table shows that the largest amount of charge transfer among neutral systems belongs to the Al(N)-BNNS/CH_4. It seems that the more value of the obtained charge transfer in this system would be related to the considerable amount of E_{ads} of CH_4. Therefore, one can conclude that the charge transferring process should have a main contribution in E_{ads} of CH_4 on the Al(N)-BNNS.

As it can be seen, the charge injection in Al(B) and Al(N)-BNNS switches the charge transfer direction whereby the charge is transferred to the CH_4. It should be noted that when the Al(B)-BNNS is utilized as a gas sensor, escaping of the CH_4 from the surface of $1e^+$-charged nanosheet can lead to a considerable reduction of the recovery time. Moreover, the largest value of charge transfer, from CH_4 to the nanosheets, is observed for $2e^+$ state of Al(N)-BNNS/CH_4 (-0.245|e|)

possessing the largest E_{ads}. Thus, it seems that similar to the neutral state, charge transfer plays an important role in CH_4 adsorption on charge-removed Al(N)-BNNS system.

Table 3. Charge transfer (|e|) in the adsorption process of CH_4 on the BNNSs at the MPW1PW91 and the M06-2X methods

System	Charge state					
	0		-1		+1	
	MPW1PW91	M062X	MPW1PW91	M062X	MPW1PW91	M062X
BN/CH_4	0.001	0.001	0.001	0.000	0.002	0.002
$Al(B)/CH_4$	0.042	0.040	-0.062 (-0.131)[a]	-0.096 (-0.169)	0.063 (0.085)	0.061 (0.083)
$Al(N)/CH_4$	0.122	0.119	-0.032 (-0.145)	-0.036 (-0.202)	0.198 (0.229)	0.192 (0.245)
$C(B)/CH_4$	-0.026	-0.028	-0.031 (-0.13)	-0.044 (-0.032)	-0.012 (-0.011)	-0.012 (-0.012)
$C(N)/CH_4$	0.001	0.000	-0.002	-0.003	0.002	0.001
$Si(B)/CH_4$	-0.059	-0.060	-0.145	-0.148	-0.029	-0.030
$Si(N)/CH_4$	-0.037	-0.037	-0.073	-0.076	-0.017	-0.017
$P(B)/CH_4$	-0.043	-0.043	-0.047	-0.046	-0.009	-0.003
$P(N)/CH_4$	-0.024	-0.024	-0.044	-0.060	-0.016	-0.019

[a] The values given in parenthesis refer states of +2 and -2 electrical charging.

3.2.3. Structural and electronic properties of methane adsorption on the BNNSs

Other adsorption properties of the CH_4 on the BNNSs, at the two different computational levels, are reported in Table 4. As shown, protrusion of doped atom as a criterion of structure deformation of adsorbent has changed partially upon the CH_4 adsorption. Interestingly, CH_4 adsorption has no effect on the structure of the C(B)-BNNS. The mentioned configuration in which the CH_4 can adsorb on both sides of sheet, especially in $2e^+$ state, leads to an appropriate situation for the CH_4 storage.

Based on the results, a reasonable reverse relation between the absolute values of E_{ads} and the minimum equilibrium distance (D) between C atom of CH_4 and doped heteroatom has been established. For example, the smallest and largest values of D are corresponded to the largest and smallest absolute values of E_{ads}, respectively.

The charge values on the doped heteroatoms, after CH_4 adsorption on neutral states of BNNSs, were also reported in Table 4. In the most cases, according to the results obtained from both used computational levels, the doped atoms have a positive charge. Also, due to the more electronegativity of N atoms in the Y(B)-BNNS/CH_4, the charge on the doped heteroatoms is more positive than that of X(N)-BNNS/CH_4 systems. Regarding to the negative charge on the C atom (-0.54|e|) from CH_4, it is reasonable to expect that the electrostatic interactions have the significant role in the CH_4 adsorption on the Al-BNNSs. Remarkably, this idea is confirmed with the appropriate position of the CH_4 in which the C atom, interacts directly with the Al (+1.2 |e|) atom from the Al(B)-BNNS (see section 3.2.6). In addition, the minimum values of E_{ads} have been obtained for pristine BNNS and C(N)-BNNS systems in which interacting atoms with the CH_4 (N and C) have negative charges.

Table 4. Structural and electronic properties for the CH_4 adsorption on the BNNSs.

Systems	P (Å)[a]	D (Å)[b]	Charge on doped atoms (|e|)		E_{gap} variation(eV)[e] (MPW1PW91) Charging state		
			MPW1PW91	M06-2X	0	-1e	+1e
BN/CH_4	0.00	4.96	-1.053(N)[c]	-1.132	0.005	0.002	0.002
$Al(B)/CH_4$	1.09	3.20	1.181(Al)	1.197	0.002	-0.061	0.287
$Al(N)/CH_4$	2.13	2.63	0.246(Al)	0.264	0.602	-0.542	0.769
$C(B)/CH_4$	0.07	3.13	0.328(C)	0.324	0.418	0.116	-0.439
$C(N)/CH_4$	0.00	4.51	-0.723(C)	-0.753	-0.007	0.020	0.001
$Si(B)/CH_4$	1.33	3.57	0.524(Si)	0.604	0.006	0.050	0.025
$Si(N)/CH_4$	1.89	4.09	0.252(Si)	0.279	-0.011	0.032	0.008
$P(B)/CH_4$	1.29	3.55	0. 205(P)	0.232	0.006	0.00	-0.010
$P(N)/CH_4$	1.69	3.77	-0.279(P)	-0.292	0.004	0.00	-0.004

[a] the protrusion of the doped heteroatoms after CH_4 adsorption.
[b] the distance between C atom of CH_4 and doped heteroatom ($C_{Methane}$-X_{Sheet}).
[c] N atom from pristine sheet is the target of CH_4 molecule.
[d] E_{gap} refers to the energy gap between HOMO and LUMO.
[e] the $E_{gap,after}$ - $E_{gap,before}$ for CH_4 adsorption.

The values of E_{gap} for all the BNNS/CH_4 systems are also reported in Table 4. As can be seen, the possibility of the CH_4 detection is enhanced by some charging states (0, $1e^-$ and $1e^+$) of the

studied systems. According to the ΔE_{gap} values, the Al(B)-BNNS/$1e^+$ system, is the only state that may be distinguished as CH_4 detector. However, because of moderate E_{ads} and non-considerable amount of charge transfer, this case is not suitable for CH_4 detection. Both neutral and $1e^+$ states of the Al(N)-BNNS system show considerable amounts of ΔE_{gap}. According to the large amounts of both E_{ads} and charge transfer, $1e^+$ state of Al(N)-BNNS can be considered as an appropriate system for the CH_4 detection. Also, because of small amount of E_{ads} for the neutral state and low amounts of both charge transfer and ΔE_{gap} in $1e^-$ state, C(B)-BNNS system is not suggested for CH_4 detection.

The values of dipole moment of BNNS flakes and hybridization of doped atom are also calculated to consider their effect on the E_{ads} (Table 1). It is mentionable that there is good relationship between the dipole moment value of Al(B),Al(N) and C(B)-BNNSs, showing the more adsorption energy for methane adsorption, and the E_{ads}. Therefore, both of Al(B) and Al(N) cases in the positively charged state and also C(B) case in the negatively charged state, having the more dipole moment value in their systems, show the more E_{ads}. However, as can be seen from Tables 1 and 2, no explicit relations between E_{ads} and hybridization of doped atom could be understood.

3.2.4. Molecular orbital schemes

The EDD schemes can be effectively utilized for studying the adsorption behavior of the CH_4 on BNNSs. In almost all cases (Table 2), the injection or removing of charge strengthens the CH_4 adsorption. This could be explained on the basis of serious reduction of the $E_{gap,}$ and raising the probability of electronic excitations from valance band to conduction band. However, in some cases the values of E_{ads} could not be explained only on the basis of the E_{gap} variation concept. By

using the EDD, this anomalous behavior can be effectively discussed. The EDD of the HOMO, LUMO and LUMO+1 of pristine BNNS are shown in Figure 3.

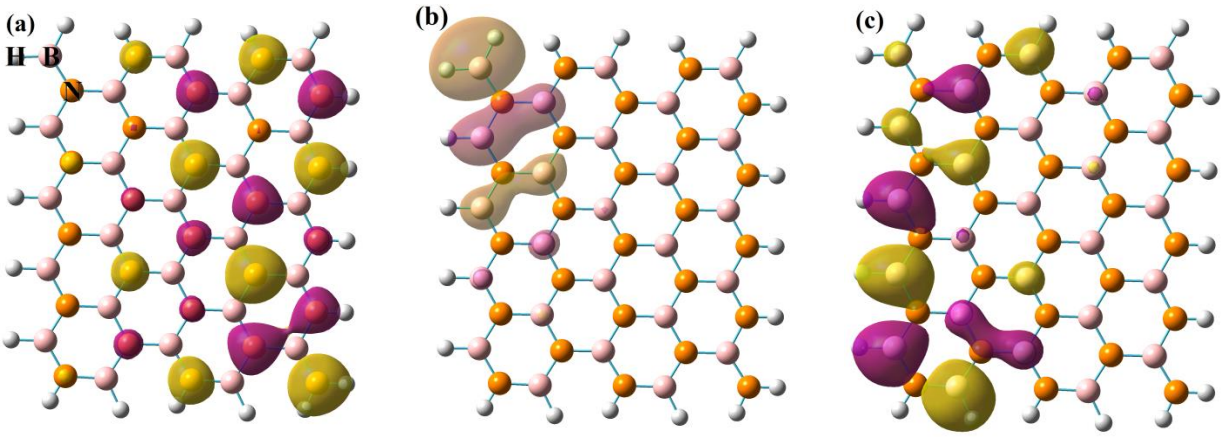

Fig. 3. The electron density distribution of (a) HOMO, (b) LUMO and (c) LUMO+1 of pristine BNNS.

As there is no overlap between the EDD of HOMO and LUMO, a small efficient presence of electrons in LUMO and thereafter a weak interaction between neutral pristine BNNS and CH_4 is expected. On the other hand instant excitation of electrons from HOMO to LUMO is limited remarkably by the large E_{gap}. This is the reason why the CH_4 does not effectively adsorb on the neutral pristine BNNS. Injection of $1e^-$ turns LUMO and LUMO+1 to new HOMO and LUMO, respectively. Because of inefficient overlap between these orbitals, despite considerable reduction of E_{gap} (Table 1), no efficient adsorption of CH_4 is observed. A similar situation occurs for $1e^+$ charging state of pristine BNNS.

The EDD of the HOMO, LUMO, LUMO+1 and a combination of LUMO+2 to LUMO+6 for the Al(B)- and Al(N)-BNNS systems are shown in Figure 4. According to this figure, in the neutral pristine state of Al(N)-BNNS in contrast with the Al(B)-BNNS system, there is a constructive overlap between HOMO and LUMO providing a suitable situation for interaction of sheet with the CH_4. Furthermore, the probability of excitation of electrons to LUMO is limited by a large amount of E_{gap} in the Al(B)-BNNS system. On the other hand, while a small overlap

between LUMO and LUMO+1 of Al(B)-BNNS was observed, no overlap between this orbitals was observed in the Al(N)-BNNS system. This explains why the CH_4 is repulsed strongly in the $1e^-$ state of Al(N)-BNNS/CH_4 system related to the Al(B)-BNNS/CH_4. Considering that other virtual MOs rather than LUMO+1 are participated in interaction with the CH4, a combination of EDD of LUMO+2 through LUMO+6 are also shown in Figure 4. As can be seen, in contrast with the Al(B)-BNNS, in the Al(N)-BNNS system, all unoccupied MOs strengthen the dispersion forces between CH_4 and BNNS through extension of EDDs on the Al atom in the Al(N) case. This might be the reason why the adsorption energy in the Al(N)-BNNS/CH_4 system is exceeded approximately 80% of the Al(B)-BNNS/CH_4, while the electrostatic charge on the Al atom in the Al(N)-BNNS/CH_4 system is smaller than half amount of that in the Al(B)-BNNS/CH_4.

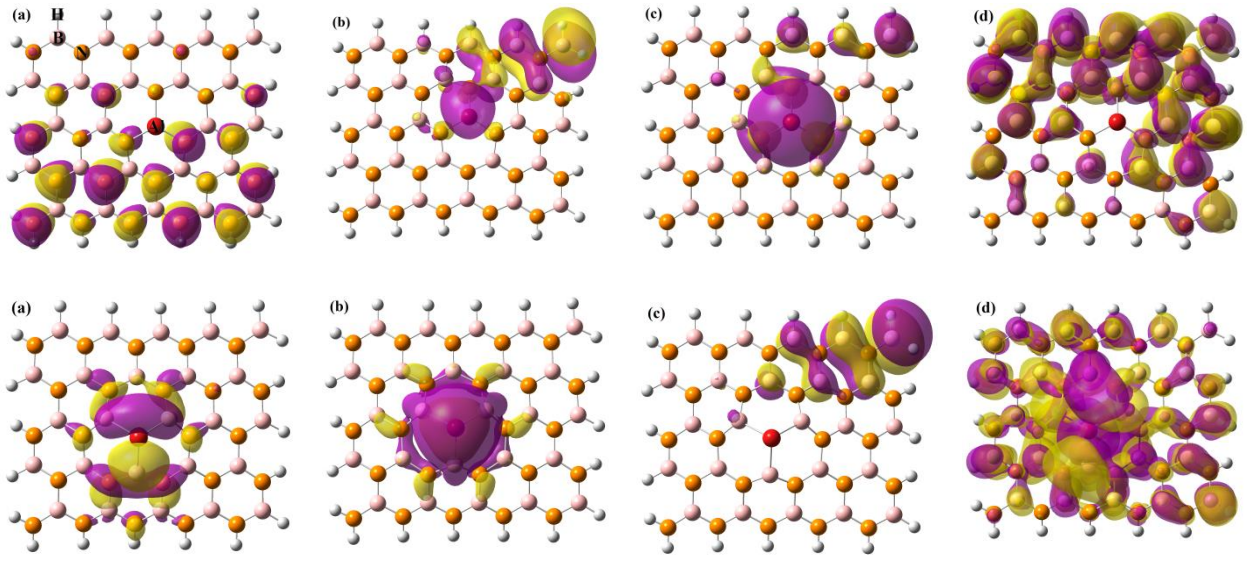

Fig. 4. The electron density distribution of (a) HOMO, (b) LUMO, (c) LUMO+1 and (d) a combination of LUMO+2 to LUMO+6 for Al(B)-BNNS (above) and Al(N)-BNNS (below).

3.2.5. DOS analysis

In order to investigate the effects of the CH_4 adsorption on density of electronic states, the PDOS analysis was utilized and extracted spectrums of selected systems were shown in Figure 5.

According to the section 3.1, to get a more realistic data, the PDOS schemes were calculated at MPW1PW91 method. These schemes are shown for those situations in which the CH_4 adsorption has a suitable value of E_{ads}, Al(B)-, Al(N)- and C(B)- BNNS systems (Figure 5). Obviously, compared with the Al(B)-BNNS system, no change was observed in the PDOS diagram of Al(B)-BNNS/CH_4. Thus, the Al(B)-BNNS system is not a suitable sensor for the CH_4 detection. For the Al(N)-BNNS system, by the CH_4 adsorption, the E_{gap} increased remarkably and the energy levels of conductance band become closer to each other. Further, the considerable amount of the charge transfer between the CH_4 and neutral nanosheet (~0.106 |e|) can support the statement that this flake is an effective sensor for the CH_4 detection. Along with increasing of the E_{gap} after CH_4 adsorption on the C(B)-BNNS system, an amplification was observed for the peak located around the Fermi level (Figure 5 (B1)). However, according to the results from the section 3.2.2, the C(B)-BNNS system is not suggested for the CH_4 detection.

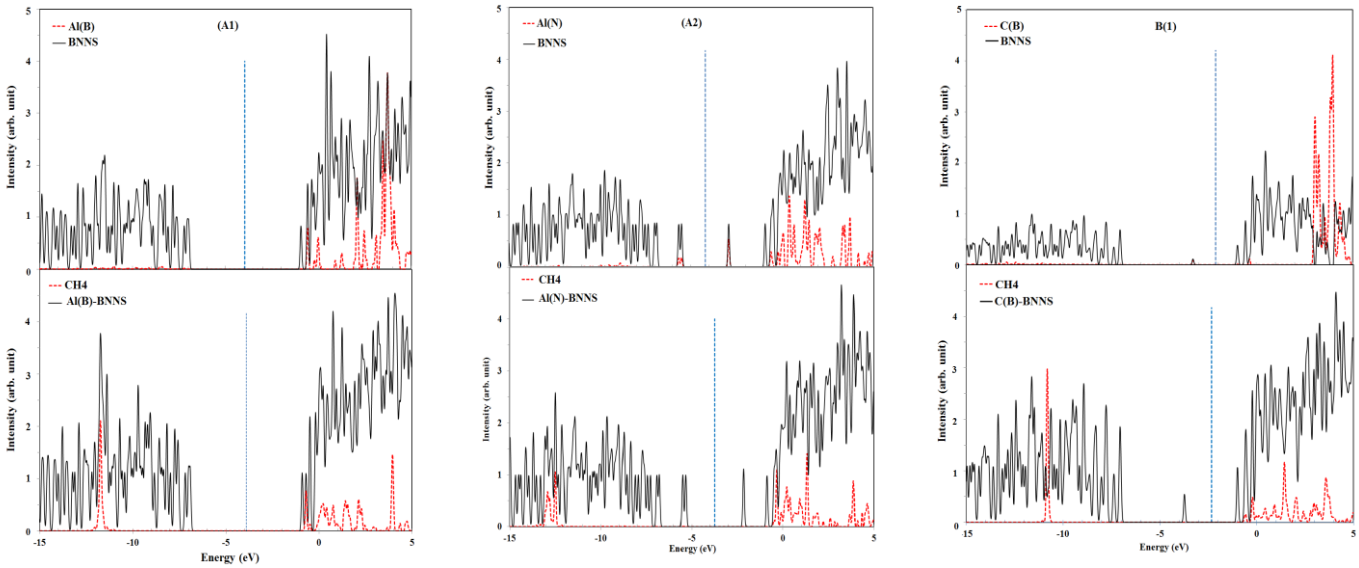

Fig. 5. The PDOS of Al(B)- (A1), A2: Al(N) and B1: C(B) doped BNNSs before (above spectrum) and after (below spectrum) CH_4 adsorption.

3.2.6. AIM analysis

To gain further insight into the nature of the interaction between the CH_4 molecule and BNNSs, the results obtained with the AIM methodology are discussed here. These results are based on topological analysis of total electric density (ρ) in critical points (CP). Notice that the nature of chemical bonds and molecular reactivity are denoted by $\rho(r)$, and its corresponding Laplacian, $\nabla^2\rho(r)$. While negative values of $\nabla^2\rho(r)$ show addition potential energy at bond critical points (BCP) which is the specialty of shared interactions (for example covalent bonds), positive values of this quantity divulge depletion of electric charge along the bond path, which is specification of closed-shell interactions (such as hydrogen bonds). According to the virial theorem at CP,[29] $\nabla^2\rho(r)$ is associated to energetic topological parameters of G_C and V_C (respectively, the kinetic and potential energy density at CP) by a local expression:

$$1/4\nabla^2\rho(r) = V(r) + 2G(r) \quad (1)$$

In addition, the $-G_C/V_C$ ratio has been used as a measure of the covalency in non-covalent interactions in which values greater than 1 generally refer a non-covalent interaction without covalent character, while ratios smaller than 1 are stating the more covalent nature of the interactions.[36] Figure 6 and Table 5 show interaction path and also data obtained by the AIM analysis. As indicated, in all the studied systems but Al(B)-BNNS/CH_4, the interactions of hydrogen atom of the CH_4 molecule with the doped heteroatoms on the surface of BNNSs(N atom from pristine BNNS) are dominant. Remarkably, in the Al(B)-BNNS/CH_4 system, the interaction between the C atom from CH_4 and the Al atom from sheet (Al…C) plays the more important role.

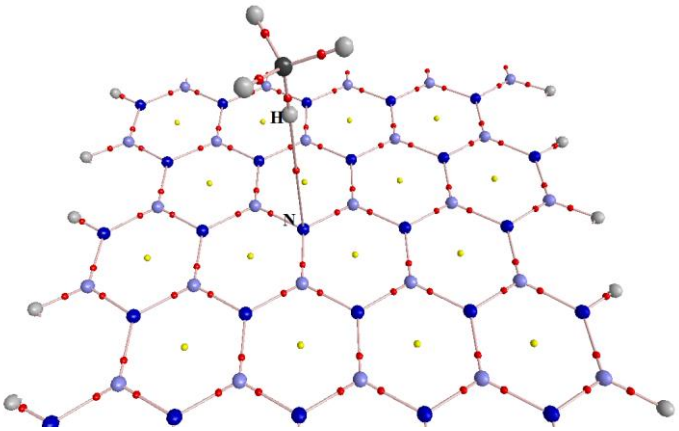

BNNS/CH_4

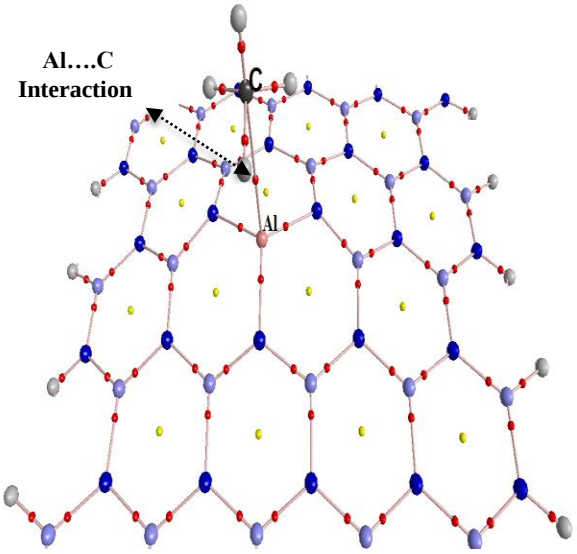

Al(B)-BNNS/CH_4

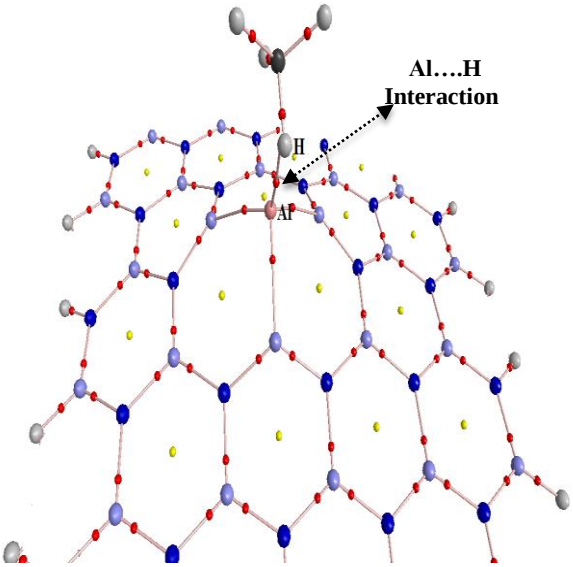

Al(N)-BNNS/CH_4

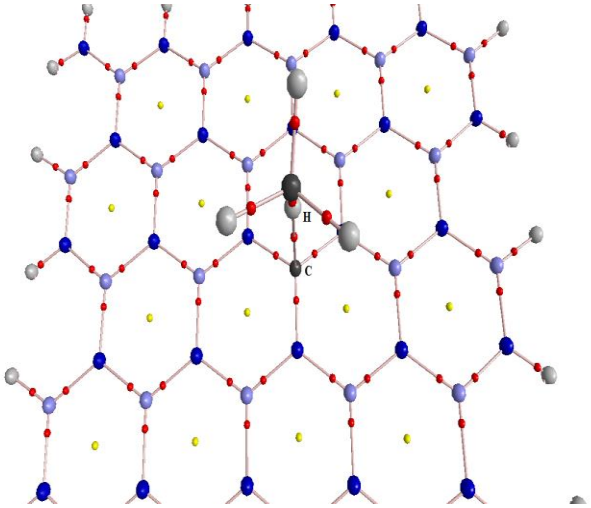

C(B)-BNNS/CH_4

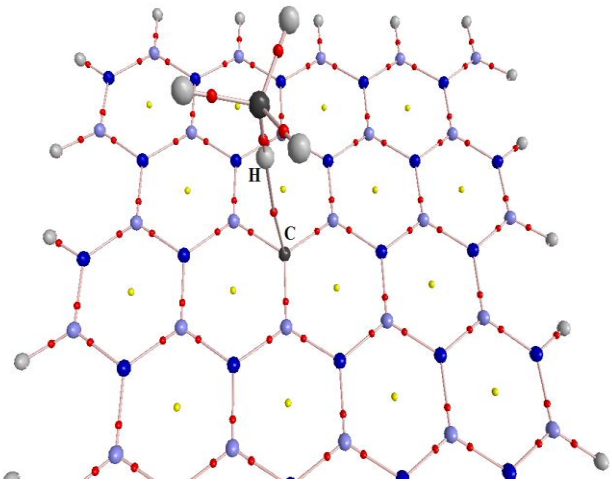

C(N)-BNNS/CH_4

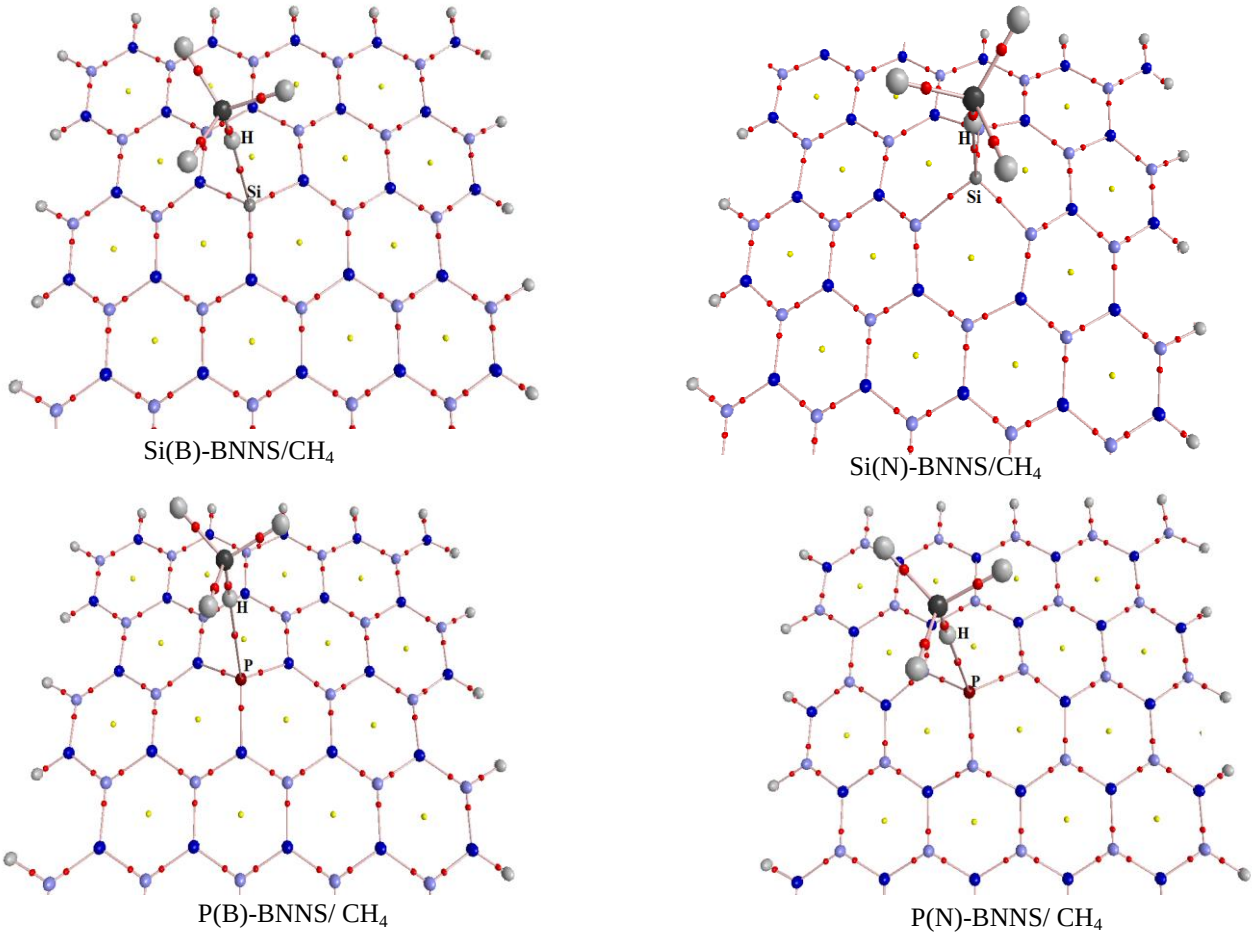

Fig. 6. The representation of molecular graph of all considered systems by AIM analysis. The red and yellow dots represent the position of the bond and ring critical points, respectively.

It is noteworthy to mention that among all CH_4-nanosheet interactions, the maximum values of the $\rho(r)$ and $\nabla^2\rho$ (r) from one hand and also the minimum values of the interaction distance and the -G(r)/V(r) ratio on the other hand, are belonged to the interaction in the most stable system, Al(N)-BNNS/CH_4. It is also shown that the -G(r)/V(r) ratio for the other cases are greater than unity which shows that the interactions have a noncovalent nature in these systems. Considering the data obtained for the systems in which the CH_4 shows the more E_{ads} (Al(B),Al(N) and C(B)-BNNSs), there are good correlation relationships between adsorption energyand each of ρ_{BCP},or $\nabla^2\rho_{BCP}$, Figure.7. As seen in these systems, the more values of the ρ (0.0190, 0.0054 and 0.0037 a.u) and $\nabla^2\rho$ (0.0348, 0.0123 and 0.0080 a.u) are obtained for the systems with the more E_{ads}.

Table 5. Interatomic distances (Å) and bond critical point data (a.u) calculated for all the systems

System	Interaction	Distance	ρ	$\nabla^2\rho$	-G/V
BN/CH_4	N....H	3.874	0.0007	0.0027	1.8864
$Al(B)/CH_4$	Al...C	3.200	0.0054	0.0123	1.1750
$Al(N)/CH_4$	Al...H	2.163	0.0190	0.0348	0.8129
$C(B)/CH_4$	C….H	3.133	0.0037	0.0080	1.1092
$C(N)/CH_4$	C….H	4.518	0.0002	0.0008	1.1051
$Si(B)/CH_4$	Si....H	3.573	0.0031	0.0062	1.2459
$Si(N)/CH_4$	Si....H	4.001	0.0010	0.0026	1.6245
$P(B)/CH_4$	P.....H	3.551	0.0028	0.0070	1.4143
$P(N)/CH_4$	P.....H	3.788	0.0017	0.0046	1.5621

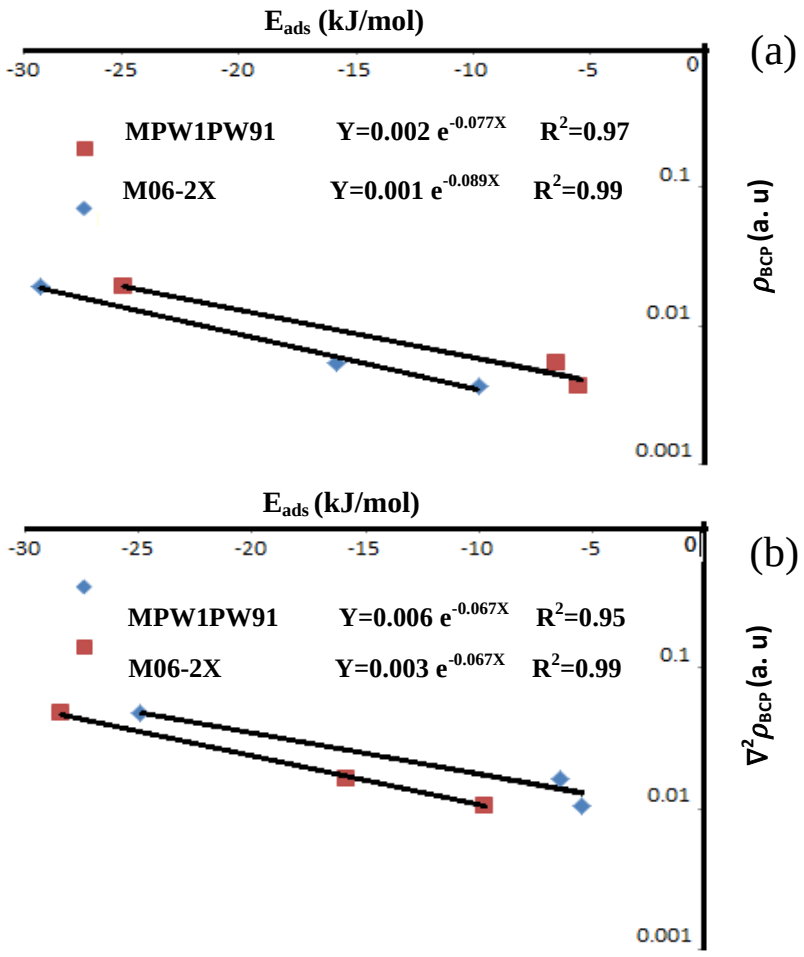

Fig. 7. The exponential relationships between adsorption energies and (a) ρ_{BCP}, (b) $\nabla^2\rho_{BCP}$ (a.u.). The systems in which the CH_4 shows the more E_{ads} (Al(B),Al(N) and C(B)-BNNSs) are considered here.

A closer look at the results shows also that the smaller distances are correlated with larger values of ρ(r) and $\nabla^2\rho$(r). Previous reports have shown that this correlation should be exponential.[37] As shown by Figure 8, there is a good exponential relationship between interatomic distances of the interacting species and each of ρ(r) and $\nabla^2\rho$(r) quantities.

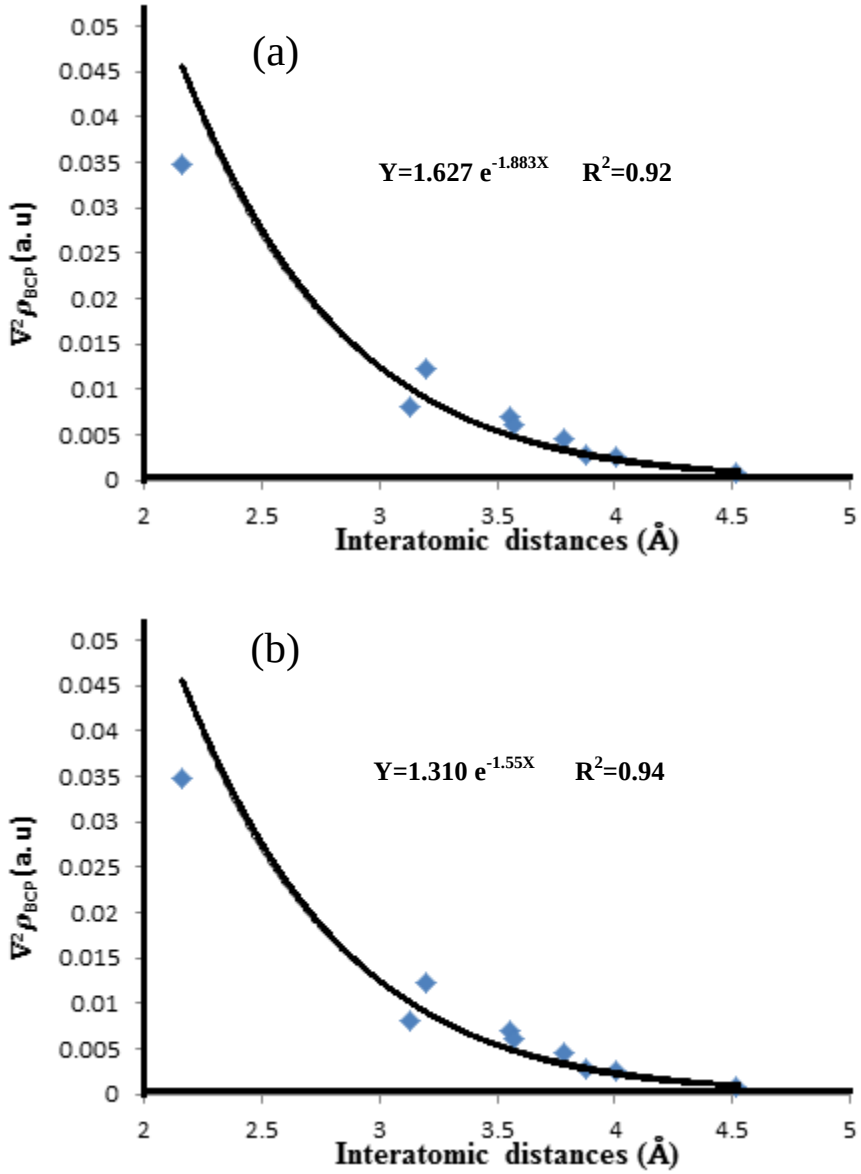

Fig. 8. The obtained exponential relationships between the interatomic distances (Å) and the (a) ρ_{BCP}, (b) $\nabla^2\rho_{BCP}$ (a.u.). All intermolecular interactions between two moieties are considered here.

4. Conclusion

We have studied the CH_4 adsorption on pristine, Al, C, Si and P-BNNSs via DFT calculations. The energy of adsorption, geometry and electronic properties including charge transfer, energy gap, PDOS and AIM analyses of all the CH_4-adsorbed systems have been calculated and analyzed. Firstly, it has been shown that CH_4 cannot effectively bind to the surface of the pristine or C-, P- and Si- doped BNNSs. On the other hand, the neutral state of both Al(B)- and Al(N)-BNNS systems are promising candidate for the CH_4 storage. The corresponding results show that the Al(N)-BNNS/CH_4 system gives the more adsorption energy related to Al(B)-BNNS/CH_4 and the charge transfer plays an important role in the process. While, the dipole moment of BNNS and hybridization of doped atom have no effect on CH_4 adsorption, a moderate amount of concentrated positive charge and considerable electron density on doped atom along with small E_g of BNNS are favorable requirements for the adsorption of CH_4 on doped BNNSs. From energy data we have theoretically found that the capacity of CH_4 adsorption on some of BNNSs can be drastically enhanced by introducing or extracting the electrons. As a consequence, a good charge-controlled switchable CH_4 storage on the Al(N)- and C(B)-BNNSs was observed. More importantly, the Al(N)-BNNT/$2e^+$ case was seen to be the more attractive for the CH_4 storage, by the maximum value of the adsorption energy (78.73 $kJ.mol^{-1}$). The results obtained from the AIM analysis show that among all CH_4-nanosheet interactions present in this work, the maximum values of the $\rho(r)$ and $\nabla^2\rho$ (r) along with the minimum values of the -G(r)/V(r) ratio are belonged to the most stable system, Al(N)-BNNS/CH_4.

References

1 B. McEnaney, T. J . Mays and X. Chen, *Fuel*, **1998**, 77, 557.

2 H. Tanaka. E. El-Merraoui, W. A. Steele and K. Kaneko, *Chem. Phys. Lett*, **2002**, 352, 334.

3 E. Bekyarova, K. Murata, M. Yudasaka, D. Kasuya, S. Iijima, H. Tanaka, H. Kahoh and K. J. Kaneko, *Phys. Chem. B*, **2003**, 107, 4681.

4 D. Cao, X. Zhang, J. Chen, W. Wang and J. Yun, *J. Phys. Chem*. *B* **2003**, 107, 13286.

5 D. Y. Kim, C.M. Yang, H. Noguchi, M. Yamamoto, T. Ohba, H. Kanoh and K. Kaneko, *Carbon*, **2008**, 46, 611.

6 N. Kumar, K. S. Subrahmanyam, P. Chaturbedy, R. Kalyan, A. Govindaraj, K. P. Hembram, A. K. Mishra, U. V. Waghmare and C. N. R. Rao, *Chem Sus Chem*, **2011**, 4, 1662.

7 Z. Mahdavifar and M. Haghbayan, *App. Surf. Sci*, **2012**, 263, 553.

8 M. Darvish Ganji, A. Mirnejad and A. Najafi, *Sci. Technol. Adv. Mater*, **2010**, 11, 9.

9 K. Azizi, K. Salabat and A. Seif, *App. Surf. Sci*, **2014**, 309, 54.

10 A. Granja, J. A. Alonso, I. Cabria and M. J. López, *RSC* Adv, **2015**, 5, 47945.

11 Z. M. Ao, J. Yang, S. Li and Q. Jiang, *Chem. Phys. Lett*, **2008**, 461, 276.

12 H. Zhang. X. Luo, X Lin. X Lu and Y Leng, *Iner. J. hydro. energy*, **2013**, 38, 1469.

13 Y.H. Zhang, K.G Zhou, X.C. Gou, K.F. Xie, H.L. Zhang and Y. Peng, *Chem. Phys. Lett*, **2010**, 484, 266.

14 S. Ma, *Adv. Mater. Res*, **2011**, 197, 701.

15 W. Zhao and Q. Y. Meng, *Adv. Mate. Res.*, **2013**, 602,870.

16 M. Seyed-Talebi and M. Neek-Amal, *J. Appl. Phys.* **2014**, 116, 153507.

17 Y. Jiao, Y. Zheng, S. C. Smith, A. Du and Z. Zhu, *Chem. Sus. Chem*, **2014,** *7*, 435.

18 S. W. de Silva, A. Du, W. Senadeera and Y.Gu, *Beilstein J. Nanotechnol*, **2014**, 5, 413.

19 Q. Sun, Z. Li, D. J. Searles, Y. Chen, G. M. Lu and A. Du, *J. Am. Chem. Soc*. **2013**, 135, 8246.

20 M.W. Schmidt, K. K. Baldridge, J.A. Boatz, Elbert, S.T. MS. Gordon, J. H. Jensen, S. Koseki, N. Matsunaga, K. A. Nguyen, S. J. Su, T. L. Windus, M. Dupuis and J. A. Montgomery, Gamess Version 11. *J. Comput Chem*. **1993**, 14, 1347.

21 J.P. Perdew and Y. Wang, *Phy. Rev. B*, **1992**, 45, 13244.

22 W.B. De Almeida, *J. Braz. Chem. Soc*, **2005**, 16, 345.

23 J. Lan, D. Cheng, D. Cao and W. Wang, *J. Phy. Chem. C*, **2008**, 112, 5598.

24 C. Adamo and V. Barone, *J. Chem. Phys*, **1998**, 108, 664.

25 H. Arslan and O. Algul, *Spectrochim. Acta*, **2008**, 70, 109.

26 Y. Zhao, N. E. Schultz and D. G. Truhlar, *J. Chem. Theo. Comput*, 2006, 2, 364.

27 (*a*) U. C. Sing and P. A. Kollman, *J. Comput. Chem.*, **1984**, 5,129. (*b*) B. H. Bezler, K. M. Mertz and P. A. Kollman, *J. Comput. Chem.*, **1990**, 11, 431.

28 N. M. O'Boyle, A. L. Tenderholt and K.M. Langner, *J. Comput. Chem*, **2008**, 29,839.

29 R. F. W. Bader, *Atoms in Molecules: A Quantum Theory*, Clarendon press, Oxford, **1990**.

30 F. Biegler-Konig and J. Schonbohm, *AIM2000 Program Package, Ver. 2.0,* University of applied sciences, Bielefeld, **2002.**

31 M. Haque Khan, Z. Huang, F. Xiao, G. Casillas, Z. Chen, P. Molino and H. Kun Liu, *Sci*. *Rep*, **2015**, 5, 9547.

32 X. Wei, M. S. Wang, Y. Bando and D. Golberg, *ACS NANO*, **2011**, 5, 2916.

33 W. Q Han, L. Wu, Y. Zhu, K. Watanabe and T. Taniguchi, *Appl. Phys. Lett*, **2008**,93, 223103.

34 C. Zhi, Y. Bando, C. Tang, H. Kuwahara and D. Golberg *Adv.Mater*, **2009**, 21, 2889.

35 R.G Parr, W. Yang, *Density functional theory of atoms and molecules*, Oxford University Press, Oxford, **1989**.

36 M. Ziołkowski, S. J. Grabowski and J. Leszczynski, *J. Phys. Chem. A*, **2006**, 110, 6514.

37 O. Picazo, I. Alkorta and J. Elguero, *J. Org. Chem*, **2003**, 68, 7485.

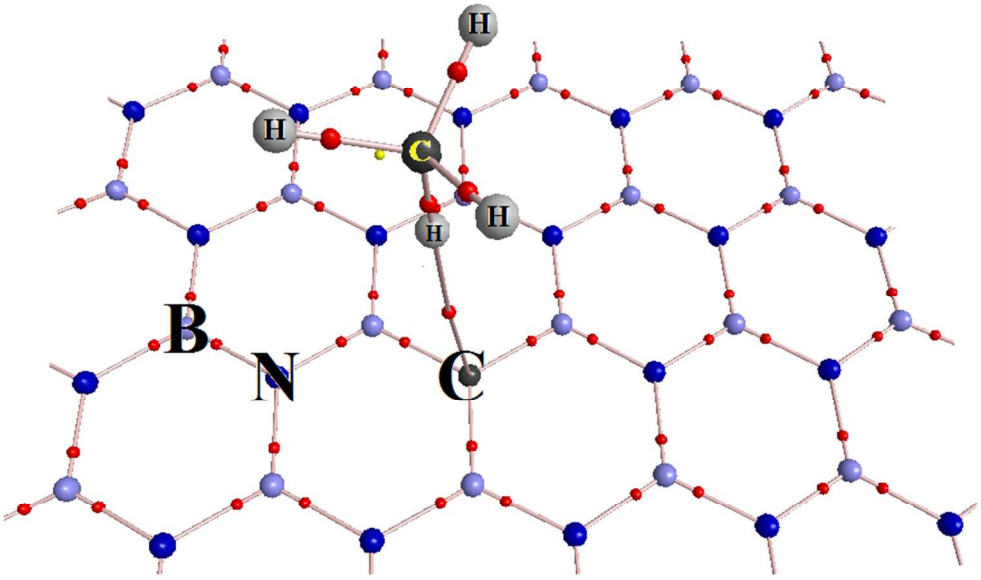

236x147mm (96 x 96 DPI)